

Photoluminescence quenching at a polythiophene/C₆₀ heterojunction

M. Theander

Laboratory of Applied Physics, Department of Physics (IFM), Linköping University, S-581 83 Linköping, Sweden

A. Yartsev, D. Zigmantas, and V. Sundström

Department of Chemical Physics, Lund University, S-221 00 Lund, Sweden

W. Mammo and M. R. Andersson

Department of Polymer Technology, Chalmers University of Technology, S-412 96 Göteborg, Sweden

O. Inganäs

Laboratory of Applied Physics, Department of Physics (IFM), Linköping University, S-581 83 Linköping, Sweden

(Received 26 October 1999)

Quenching of photoluminescence in a substituted polythiophene in the presence of a deposited C₆₀ layer is studied by steady-state and time-resolved photoluminescence (PL). The steady-state PL is evaluated by considering the interference of the absorbed and emitted electro-optical field in the thin film coupled to exciton diffusion in the conjugated polymer. PL quenching occurs for excitons generated within 5 nm from the heterojunction. A blueshift of the polymer emission spectrum is observed when C₆₀ is deposited on top of a polymer thin film. The blueshift is shown to be caused by PL quenching before the excitation is transferred to the lowest-energy sites.

INTRODUCTION

Photovoltaic devices made from conjugated polymers and C₆₀ molecules have attracted much interest due to the efficient charge separation of excitations between conjugated polymers and C₆₀. Following absorption of photons in the polymer, electron transfer from the polymer to C₆₀ occurs in the subpicosecond range while the back transfer is on the order of milliseconds.¹ This makes the charge separation very efficient and promises efficient charge collection at contacts of devices made of polymer-C₆₀ blends or heterojunctions. Small amounts of C₆₀ mixed with conjugated polymers can quench the photoluminescence by a few orders of magnitude, but in such systems the charge collection at the contacts is hampered by the formation of isolated C₆₀ regions which are not connected to the electron-collecting contact. In order to make a continuous path of C₆₀ to the electron-collecting contact, the C₆₀ content must be close to 50%. The performance of polymer/C₆₀ diodes is therefore much dependent on the morphology of the blend. Polymer/C₆₀ heterojunctions have the advantage of being much better defined than blends due to the continuous hole and electron transport path to the contacts. In addition, the well-defined interface is suitable for studying the charge separation process. As the excitation transfer between the conjugated chains occurs in picoseconds,^{2,3} faster than the lifetime of the excitons, the excitons have time to diffuse from the bulk of the polymer material to the interface of polymer/C₆₀ where the charge separation occurs. The electron transfer is dependent on the electron transfer range, i.e., the transfer rate depends on the overlap of the electronic wave functions of donor and acceptor, and since the electron wave function falls off exponentially with separation of donor and acceptor, the transfer rate will follow the same distance dependence. Several authors

have used the polymer/C₆₀ interface to estimate the diffusion range in conjugated polymers.⁴⁻⁶ In devices made of polymer/C₆₀ heterojunctions, the interpretation is made more difficult due to the mode structure of the incident optical electric field, which can either enhance or decrease the field at the interface of polymer/C₆₀, due to the presence of a highly reflecting contact (usually aluminum) and also the absorption of photons in C₆₀ contributing to the photocurrent. In order to decouple the quenching process from the device performance we have performed photoluminescence quenching experiments on polymer/C₆₀ heterojunctions.

EXPERIMENTAL METHOD

Details of the synthesis of poly{3-[4'-(1'',4'',7''-trioxaoctyl)phenyl]thiophene} (PEOPT), shown in the inset of Fig. 1, can be found elsewhere.⁷ Thin films were made by spin-coating filtered ($\phi=0.45\ \mu\text{m}$ pore size) polymer solutions (chloroform) on top of quartz substrates. The polymer film thickness was controlled by varying the polymer concentration (10–0.46 mg/ml) but keeping the spin speed constant (1000 rpm). Solvent was removed from the films by placing samples in dynamical vacuum ($P<1\times 10^{-6}$ Torr) for 1 h. For the thick polymer films, thicknesses were measured with a Dektak 3030 profilometer. The surface roughness of the quartz substrate was measured with atomic force microscopy and found to be about 1–2 nm. The polymer/air surface was also smooth and had a surface roughness similar to that of the quartz substrate. The C₆₀/polymer interface was studied with ellipsometry and was found to be sharp.⁶ A thin layer (<5 nm) of C₆₀ molecules was evaporated ($P<1\times 10^{-6}$ Torr) on part of the polymer film. As the C₆₀ covered only part of the polymer film, the photoluminescence (PL) of the polymer with and without C₆₀ could be measured with

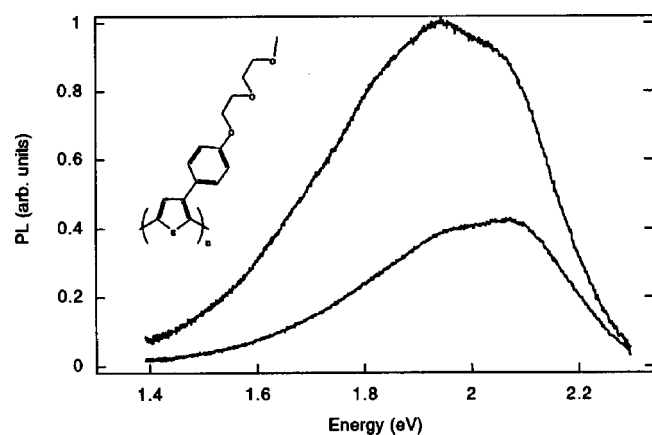


FIG. 1. PL spectra of a 7.3 nm polymer film with and without a 4 nm C_{60} layer on top (the intensity from the polymer film with C_{60} on top is lower). The chemical structure of poly{3-[4'-(1'',4'',7''-trioxaoctyl)phenyl]thiophene} (PEOPT) is given on the left side.

only a small translation of the sample, thus making errors due to sample variations small. The complex index of refraction, $n = \eta + i\kappa$, for the polymers and C_{60} was measured with spectroscopic ellipsometry (J. A. Wollam Co., Inc.). Optical absorption spectra were measured on a Perkin-Elmer $\lambda 9$ spectrometer. Steady-state emission spectra were collected by exciting the samples with monochromatized light centered at 2.34 eV from a tungsten lamp, and detecting the emission with an Oriel Instaspec IV diode matrix spectrometer. Time-resolved fluorescence spectra were measured by exciting with 3.1 eV radiation from a cw mode-locked and frequency-doubled Ti:sapphire laser generating 80 fs pulses [full width at half maximum (FWHM)]. A Hamamatsu streak camera (FESCA) with an apparatus response function of 1.3 ps (FWHM) was used to collect the time-resolved spectra. To avoid degradation, samples were put in a box (using the quartz substrate as window with polymer layer facing into the box) and flushed with nitrogen for 5 min prior to excitation. Excitation was performed with *s*-polarized light through the substrate at 45° and the emission was collected normal to the substrate surface.

RESULTS AND DISCUSSION

Photoluminescence spectra of a thin (7.3 nm) polymer film with and without C_{60} on top are shown in Fig. 1. The quenching of the PL for the sample with C_{60} on top is obvious and is attributed to efficient electron transfer from the polymer donor to the C_{60} acceptor.⁸ The PL spectrum of the neat film is redshifted by 0.2 eV with respect to the PL spectrum of the same polymer in solution.⁹ The different shape of the PL spectrum in the film (broad) compared to that found in solution (narrower transition with clear vibronic progression) indicates that emission from aggregates contributes to the steady-state PL in films. The PL spectrum is blueshifted relative to the spectrum of the film without C_{60} , when C_{60} is deposited on top of the polymer film. In Fig. 2 absorbance spectra of polymer films with and without C_{60} are shown for different polymer thicknesses. Absorbance spectra are broad and structureless and no or very little long-range order is expected in these spin-coated films. For an-

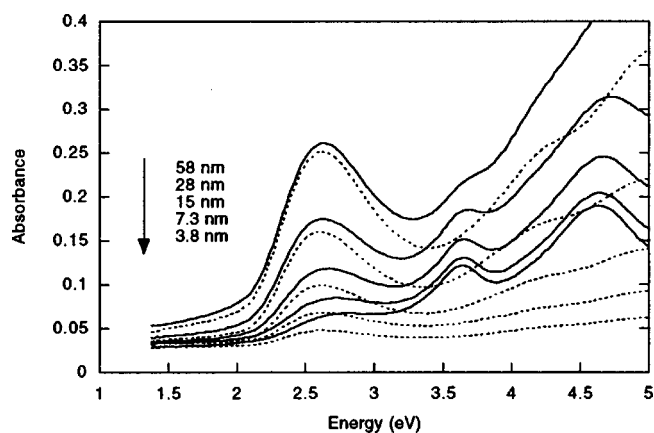


FIG. 2. Absorbance spectra of polymer films of varying thicknesses (dotted lines) as well as for the same samples with a 4 nm C_{60} layer on top (solid lines).

nealed films, the absorbance and emission spectra are much redshifted due to a planarization of the main chains, indicating a much higher intermolecular interaction.⁹ The long red tail in the absorbance spectra for energies below 2.1 eV is due to reflections at the different interfaces air-substrate-polymer- C_{60} . By using the complex index of refraction ($n = \eta + i\kappa$) as obtained from ellipsometry for the polymer, C_{60} , and the substrate, we simulate the absorbance spectra and can from that extract the polymer thickness. Thicknesses extracted from linear absorption showed good agreement with thicknesses obtained from the profilometer measurement (for thick films where the profilometer could be used) and the red tail is also reproduced. We observe that thicknesses extracted from the linear absorption of the film scale linearly with the concentration of the solution used for spin-coating the film.

The relative quenching, i.e., the reduction of the number of emitted photons, when C_{60} is deposited on top of the polymer film, normalized to the number of emitted photons of the neat polymer film, is shown in Fig. 3. When the polymer film thickness is decreased, a larger portion of the total number of excited states can reach the polymer/ C_{60} interface and hence the relative quenching increases. We have modeled the quenching process of the excited states inside the polymer layer by using a one-dimensional continuity equation as

$$\frac{\partial n(z,t)}{\partial t} = -\frac{n(z,t)}{\tau_0} + D \frac{\partial^2 n(z,t)}{\partial z^2} - S(z)n(z,t) + \frac{g(z,t)}{h\nu}, \quad (1)$$

where the change with time of the excited-state density $n(z,t)$ is given by an exponential decay with time constant τ_0 (intrinsic PL decay in neat film) and the second term is the one-dimensional diffusion characterized by the diffusion coefficient D . The third term describes the electron transfer at the polymer/ C_{60} interface (S is set to zero when no C_{60} is deposited on the polymer). The generation term $g(z)$ is given in W/m^3 , which, divided by the energy of absorbed photons $h\nu$, gives the rate of excited states generated per m^3 . Equation (1) is simplified by assuming an infinite surface quenching rate at the polymer/ C_{60} interface, with no z dependence. Hence, the surface quenching term in the equation can be

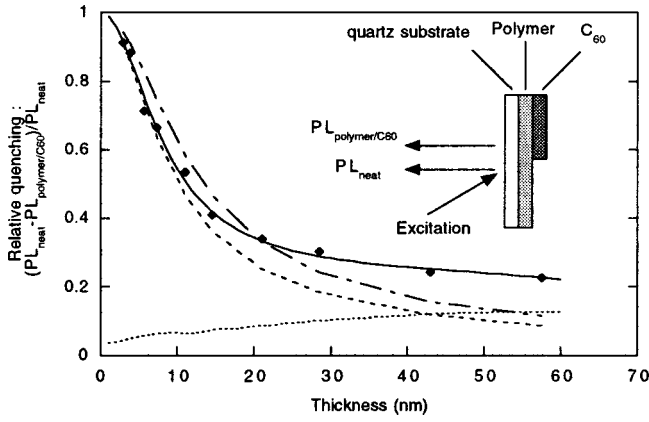


FIG. 3. The relative quenching of the polymer/ C_{60} heterojunction for different polymer layer thicknesses (diamonds), together with a fit using Eq. (2) assuming a diffusion length of 5.3 nm (solid line). For comparison, the relative quenching assuming an exponential decay of the incoming radiation (e.g., $I = I_0 e^{-\alpha z}$) for diffusion lengths 5.3 nm (dashed line) and 7 nm (broken-dashed line) are shown. Also shown is a simulation of the relative quenching assuming no quenching at the interface between the polymer and the C_{60} layer, i.e., the contribution due to interference of absorbed and emitted light (dotted line). Inset shows the sample configuration and how the sample is excited.

removed and the boundary condition $\partial n(z=d)/\partial x = -\infty$ at the polymer/ C_{60} interface is used, for polymer thickness d . At the polymer/air and substrate/polymer interfaces the surface quenching is assumed to be low and the boundary condition $\partial n/\partial x = 0$ is used.

As the excitation is impinging through the quartz substrate, as shown in Fig. 3, there will be a considerable amount of interference when light is reflected at the polymer/air interface and a pure exponential decay of the excitation light inside the polymer film is not expected. Therefore, the distribution of excitons generated inside the film with and without C_{60} is calculated by taking the derivative of Poynting's vector with respect to distance inside the polymer film z , giving

$$g(z) = \frac{c \epsilon_0 \alpha \eta}{2} \left[\left| E_+(0) \right|^2 e^{-\alpha z} + \left| E_-(0) \right|^2 e^{\alpha z} + 2 \left| E_+(0) E_-(0)^* \right| \cos\left(\frac{4\pi\eta}{\lambda} z + \gamma\right) \right], \quad (2)$$

where $E_+(0)$ and $E_-(0)$ are the calculated electric fields in the polymer film at the polymer/quartz interface ($z=0$) traveling from the interface into the polymer film (plus sign) and through the interface into the substrate (minus sign). $E_-(0)^*$ is the complex conjugate of $E_-(0)$. The absorption coefficient is denoted by α , η is the real part of the polymer refractive index, and γ is the relative phase between $E_+(0)$ and $E_-(0)^*$. With an angle of incidence other than normal, Eq. (2) will be modified, but still the z dependence can be expressed by the two exponential functions and the cosine term. The electric field is calculated assuming that no interference is present throughout the 2 mm quartz substrate (only incoherent transmission), whereas there is interference in the thin polymer and C_{60} layers.

As the emitted light is detected through the substrate, the emitted light will be modulated by interference in much the same way as the absorbed light. To model the interference of the emitted light, we assume, at a position z within the polymer film, two plane waves with amplitudes E_0 emitted (coherently) in the positive and negative z directions. For the simplest case with only one reflecting interface with reflection coefficient r at the polymer/air interface, the intensity emitted through the substrate will be proportional to

$$I(z) \propto |E_0 + E_0 r e^{2i(2\pi\eta/\lambda)(d-z)}|^2 = |E_0|^2 \left[1 + |r|^2 + 2|r| \cos\left(\frac{4\pi\eta}{\lambda}(d-z) + \varphi\right) \right], \quad (3)$$

where φ is defined as $r = |r| e^{i\varphi}$, and E_0 is the plane wave emitted from the polymer emitter at a distance z from the substrate/polymer interface. The electric field traveling toward the substrate, E_0 , will interfere with the field reflected at the polymer/air interface, $E_0 r e^{4i\pi\eta(d-z)/\lambda}$, hence giving a strong modulation of the transmission of light generated at different positions within the polymer film. We have defined the transmission of light generated at the position z within the polymer film with intensity $I_0 = |E_0|^2$ as $I(z)/I_0$, where the intensity $I(z)$ is a plane wave traveling in the negative z direction (in Fig. 4) through the quartz substrate (note that a transmission larger than unity is feasible). In the real simulation, a full analysis with all interfaces is taken into account.

When fitting the steady-state data to Eq. (1) we can set the time derivative to zero and assume an infinite quenching rate at the polymer/ C_{60} interface. The only fitting parameter will then be the diffusion length defined as

$$L_d = \sqrt{D\tau_0}. \quad (4)$$

The best fit (displayed in Fig. 3, solid line) is obtained for a diffusion length of 5.3 nm. If the interference inside the thin films is neglected and an exponential attenuation of the light intensity inside the film is assumed, the data points cannot be fitted with the same precision. This is shown in Fig. 3 for two different exciton diffusion lengths (5.3 and 7 nm). The dotted line in Fig. 3 shows a simulation of the resulting signal if no exciton quenching occurs at the polymer/ C_{60} interface. The lowering of the PL signal is thus due to interference effects in the thin film.

In the lower panel of Fig. 4 the optical mode structure is shown, for light incident from the substrate side (at 45° to the substrate normal), inside a 60 nm polymer film. Two effects due to interference are found. First, the absorption at the polymer/ C_{60} or polymer/air interface is higher than at the substrate/polymer interface, which is certainly not the case when an exponential decay of the absorbed light is assumed. Second, the absorption in the polymer will be lower when C_{60} is deposited on the film due to an additional phase shift and absorption of the reflected beam. With thicker C_{60} films the differences will increase. In the top panel of Fig. 4 the transmission of light generated at different positions in the polymer film is shown. Light generated close to the polymer/air interface has much higher transmission than light generated further away from the polymer/air interface. The strong modulation can be understood by considering the high refractive index (1.8) of the PEOPT film at the emission wave-

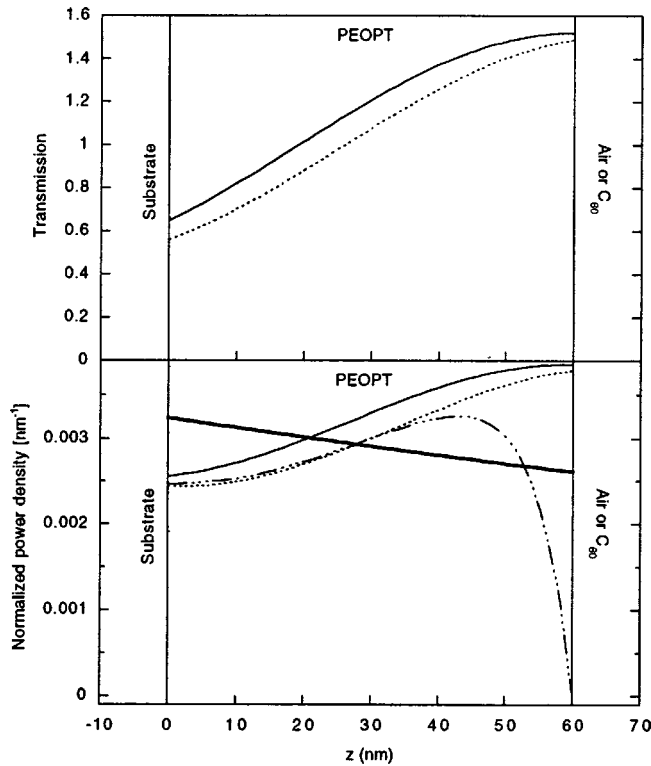


FIG. 4. The lower panel shows the calculated power excitation density $g(z)$ of a 60 nm polymer film excited at 2.34 eV, normalized to the incoming intensity. The axes thus show the fraction of the incoming intensity absorbed per length unit. The different lines are the absorbed power density for a neat film (thin solid line) and a polymer film with a 4 nm film of C_{60} on top (dashed line). The excitation density assuming an exponential decay of the incoming radiation (e.g., $I = I_0 e^{-\alpha z}$) is shown (thick solid line). Also shown is the steady-state power density with an infinite sink at the polymer/ C_{60} heterojunction and a diffusion length of 5.3 nm (broken-dashed line). The upper panel shows the calculated transmission of the polymer emission from different points z in the polymer film, to a point outside the quartz substrate (see text for more details). The transmission is shown for the case of a neat polymer film (thin solid line) and a polymer film with 4 nm C_{60} on top (dashed line).

length (2.07 eV), which will give a reflection coefficient of 0.28 at the polymer/air interface. An estimate of the maximum transmission, using Eq. (3), then gives $I(z=d)/I_0 = (1 + 0.28)^2 = 1.63$ for an emitter at the polymer/air interface and a transmission of $I(z=d-60)/I_0 = 0.72$ for an emitter at a distance of 60 nm from the polymer/air interface. In Fig. 4 the transmission is somewhat different as multiple reflections inside the structure are used in the calculations. In total, the effect of the interference will be a much higher sensitivity to the absorption and emission processes close to the polymer/ C_{60} or polymer/air interface, which is desired in the experiment.

The PL decay of a 5.6 nm neat polymer film with and without C_{60} on top detected at 2.07 eV is shown in Fig. 5. With a C_{60} layer evaporated on top of the polymer layer, the PL decay is much faster than for the neat film. The initial decay of the neat film has a time constant of about 50 ps and is nonexponential on longer time scales (not shown), which is indicative of a diffusional motion of excitations in the

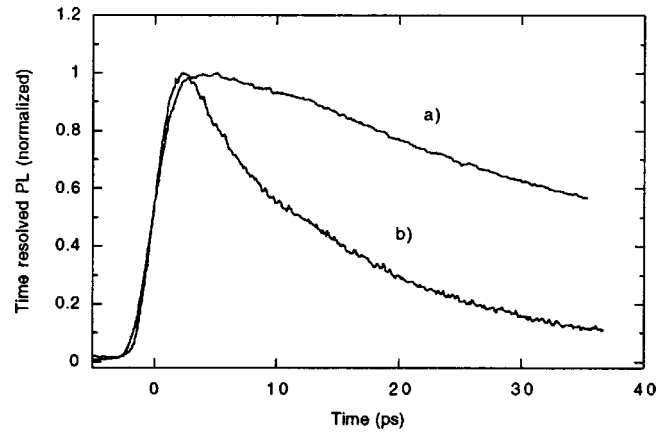


FIG. 5. Normalized PL decay of a 5.6 nm polymer film with (a) and without (b) C_{60} on top, measured at 2.07 eV.

presence of quenching sites. With C_{60} on top of the polymer, the PL decays with a time constant of only 15 ps. The faster decay of the polymer/ C_{60} film compared to the neat film must be due to quenching of excitons at the polymer/ C_{60} interface. The yield of the quenching process, Q , can be estimated from the time constants, $Q = 1 - (\tau_{\text{polymer}/C_{60}}/\tau_{\text{neat}}) = 1 - (15 \text{ ps}/50 \text{ ps}) = 0.7$. Solving Eq. (1) at steady state, we obtain an expression for the yield of the exciton quenching at the interface (assuming a constant excitation density across the polymer layer) expressed in L and L_d where L is the thickness of the polymer layer and L_d is the exciton diffusion length:

$$Q = \frac{L}{L_d} \tanh\left(\frac{L_d}{L}\right). \quad (5)$$

Setting Q equal to 0.7 we obtain $L_d/L = 0.85$ and with $L = 5.6 \text{ nm}$ a diffusion length of 4.7 nm is found. A corresponding diffusion coefficient of $4.5 \times 10^{-3} \text{ cm}^2/\text{s}$ is obtained with the excited-state lifetime of 50 ps. The diffusion coefficient obtained is an order of magnitude lower than that obtained by Haugeneder *et al.* in a ladder-PPP poly(paraphenylene) in a similar PL quenching experiment.⁵ This is consistent with the high disorder in this material in comparison with the highly ordered ladder-PPP.

In the discussion above we have described the quenching of the excitons at the interface by an infinite sink, which is an oversimplification. A more realistic model would include an electron transfer function of Marcus type,¹⁰ i.e., an electron transfer rate decreasing exponentially with the separation of donor and acceptor. With a typical transfer length of about 1 Å the result would not change significantly. Time-resolved photoinduced absorption measurements on MEH-PPV/ C_{60} poly(2-methoxy,5-(2'-ethyl)-hexyloxy-p-phenylene-vinylene) heterojunctions indicate a much longer transfer length, which was attributed to extended delocalization of the polymer wave function.¹¹

From measurements¹² of the intrinsic persistence length of P3HT poly(3-hexylthiophene) (2.1 nm), a rough estimate of the transfer distance would be half a conjugation length, i.e., about 1 nm. Here we have omitted the fact that the spatial distribution of the polymer wave function is one di-

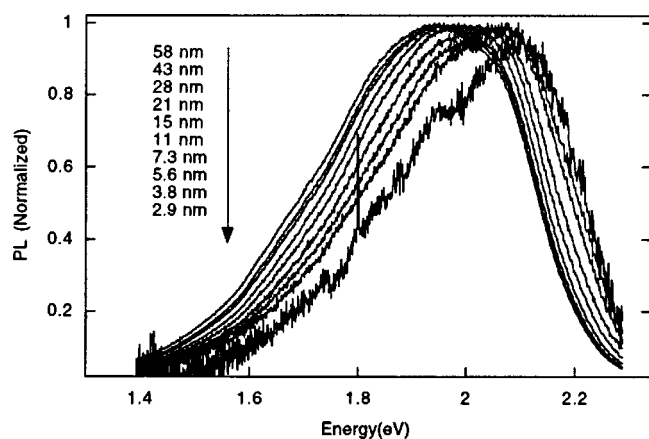


FIG. 6. Normalized steady-state PL spectra of polymer/ C_{60} double layers with varying polymer thicknesses. The C_{60} layer is approximately 4 nm for all samples.

mensional rather than three dimensional, which leads to an overestimate of the transfer distance.

The real quenching distance (in the absence of exciton diffusion) may be longer, due to a rough polymer/ C_{60} interface resulting from rough polymer surfaces as well as from penetration of C_{60} molecules to the polymer film (diffusion).¹³ We do not try to distinguish how much of the initially created exciton density is quenched on a subpicosecond time scale due to electron transfer, prior to exciton diffusion, and how much is quenched due to exciton diffusion. However, we notice that there are no signs of ultrafast decay of the PL kinetics in Fig. 5, probably implying that the fraction of directly quenched excitons is small. From the steady-state quenching data we can extract a quenching distance of ≈ 5 nm and a diffusion length presumably shorter than 5 nm.

With the C_{60} /polymer sample, the emission spectrum of the polymer is blueshifted compared to the neat film. The blueshift gradually increases as the polymer film thickness is decreased (Fig. 6). Thus, the blueshifted emission originates from polymer segments close to the polymer/ C_{60} interface and for the thickest film, with C_{60} on top, the emission spectrum is almost identical to that of the neat polymer. For the thick film, emission far from the interface will not be affected by C_{60} and hence the blueshifted emission gives only a small contribution to the total emission, and cannot be resolved.

Blueshifted polymer emission caused by the presence of C_{60} has been observed for P3HT/ C_{60} blends,¹⁴ as well as for blends of PPV (MEH-PPV) and C_{60} .¹⁵ A conformational change of the polymer backbone due to presence of C_{60} has been suggested to cause the blueshifted emission.¹⁵ In heterojunctions, the interaction between the polymer and C_{60} will be limited to the uppermost polymer layer facing C_{60} . As electron transfer has been shown to be very fast, the polymer segments in contact with C_{60} would give very little emission due to the competing electron transfer. The contribution from this interface layer to the total PL is therefore believed to be negligible. A change in the polymer conformation at the interface would therefore not explain our observation of a blueshift of the PL spectra for thin films with C_{60} on top. To investigate this hypothesis we have measured the time-resolved PL spectra. If there were an influence of

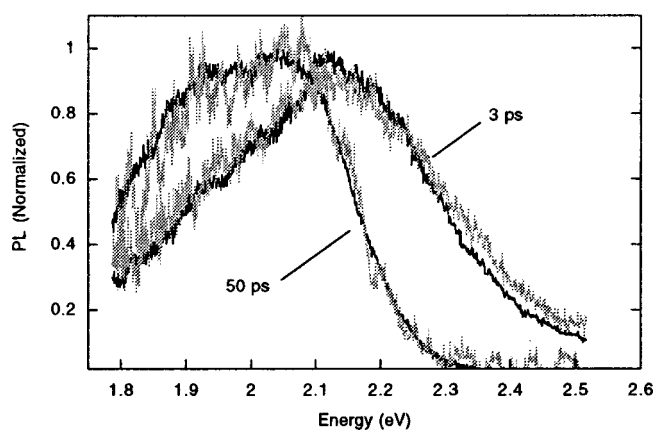


FIG. 7. Normalized time-resolved PL spectra of polymer with (gray line) and without (black line) C_{60} on top, at 3 and 50 ps after excitation with an 80 fs pulse at 3.1 eV.

C_{60} on the polymer conformation, this would be even more pronounced on short time scales when the exciton density close to C_{60} is higher. The time-resolved PL spectrum measured at 3 ps with and without C_{60} on top of the polymer film is shown in Fig. 7, and as no substantial difference can be found between the spectra a conformational change of the polymer due to the presence of the C_{60} layer can be excluded. On longer time scales, the PL spectra of the neat polymer film and of polymer/ C_{60} match each other. From this we conclude that the energy of the segment on which the excitons reside does not influence the probability of the exciton being transferred or transported toward the interface (on this time scale). By monitoring the time-resolved PL spectra at different times after excitation (Fig. 8) we see that the redshift of the spectrum is substantial even after the initially fast relaxation of 5 ps.

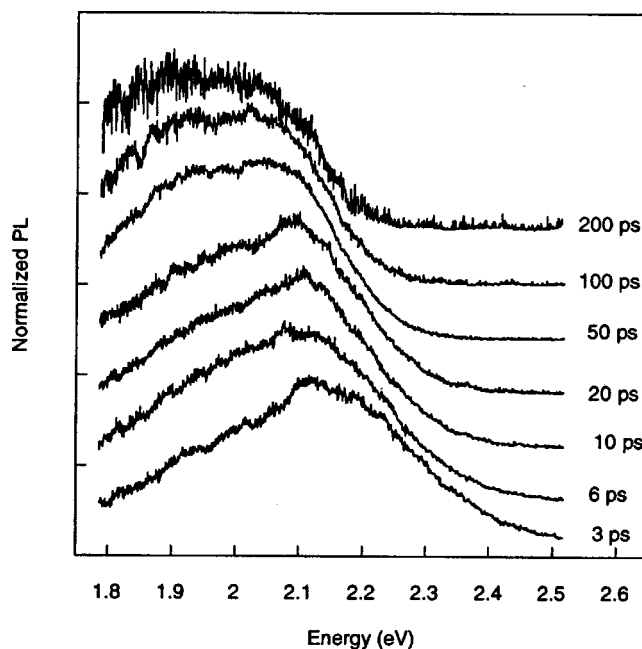


FIG. 8. Normalized time-resolved PL spectra of neat polymer film at different times after excitation with 80 fs pulse at 3.1 eV. The spectra are displaced relative to each other along the vertical axis, for clarity.

As the PL decay is much faster with C₆₀ on top of the polymer film, the reason for the blueshift of the steady-state PL spectrum of the polymer film with C₆₀ on top is the higher contribution to the time-integrated spectrum from nonrelaxed excitations with high energy. This must be a general result for polymers with broad distribution of site energies due to conjugation breaks and interchain interaction.

We can estimate the efficiency of incident photons converted to electrons (IPCE) for a polymer/C₆₀ heterojunction photodiode, based on the PL quenching distance. With the imaginary part of the refractive index $\kappa=0.276$ at 2.61 eV the absorption coefficient is $\alpha=4\pi\kappa/\lambda=7.3\times 10^4\text{ cm}^{-1}$. Together with the measured diffusion length L_d , the total amount of collected charges would be $L_d\alpha\approx 0.029$. In a device, the electron-collecting contact is usually aluminum and, with constructive interference with the reflected optical field, almost twice as much light can be generated at the interface giving a maximal IPCE of approximately 6% for a double-layer device. Recent results on such a polymer/C₆₀ heterojunction photodiode indicate a much higher IPCE, due to photocurrents originating from light absorbed in the C₆₀ layer.⁶ Careful modeling of the photocurrent action spectrum⁶ gave a diffusion length in the polymer of 4.7 nm in excellent agreement with our PL quenching experiment. The good agreement between the steady-state PL quenching distance and the quenching distance from the photodiode modeling supports our observations of a sharp interface between the polymer and C₆₀.

The absence of polymer/C₆₀ interdiffusion can be further supported by parallel studies of another polythiophene derivative. Here we know that the polymer is well miscible with C₆₀.⁷ In heterojunctions between this phenyl-substituted polythiophene {namely, poly [3-(2'-methoxy-5'-octylphenyl)thiophene]} and C₆₀, annealing of the heterojunction gives an increase of the relative PL quenching compared to that in heterojunctions that have not been annealed. The PL spectra and PL yield of the neat polymer film did not change on annealing. The polymer contribution to the photodiode IPCE made from an annealed heterojunction was lower than for the devices that were not annealed. Our interpretation of the result is that annealing makes C₆₀ diffuse into the polymer film and efficiently quench the polymer PL but the electrons cannot be collected in the device since no continuous electron conduction path is supplied by the isolated C₆₀ molecules. The isolated C₆₀ molecules act as traps which shorten the diffusion length of excitons in the polymer and reduce the performance of photodiodes made of annealed heterojunctions.

To increase the number of electron-hole pairs generated at the polymer/C₆₀ interface, we need to optimize the product

$L_d\alpha$ describing the number of excitons in the polymer film that can reach the interface. By decreasing the density of side chains relative to the conjugated backbones, the absorption coefficient can be increased. The diffusion coefficient will also increase with shorter interchain distances. Furthermore, order in the material will increase the diffusion coefficient. Ordering and close packing might also have a negative effect, by facilitating the formation of interchain excited states, which will quench the intrachain excitons. Thus the lifetime of the intrachain excitons will be lowered and the diffusion length will be reduced. An optimization of the density of side chains might then give an optimal performance. Extrinsic defects such as residual impurities as well as chemical imperfections (cross links and carbonyl formation) will reduce the PL lifetime and the purity of the material should therefore be as high as possible. The short PL lifetime (50 ps) is limiting the diffusion length of the polymer and must be due to quenching sites (extrinsic or intrinsic). Further insight into the nature of the quenching mechanism is necessary to increase the PL lifetime and the device performance in heterojunctions.

CONCLUSION

From our results, we find a PL quenching range of 5 nm in the polymer PEOPT in the presence of a C₆₀ interface. The short range is attributed to the high disorder in the material in combination with quenching traps, which prevent the exciton from diffusing long distances before being quenched by the C₆₀ interface. The quenching range agrees very well with modeling of the photocurrent in devices made of such heterojunctions. Only a small fraction of the absorbed light in the polymer in such devices contributes to the photocurrent, by being converted to free electron-hole pairs. A blueshift of the steady-state PL spectrum is a consequence of competition between the fast quenching of excitons at the polymer/C₆₀ interface and a slower spectral diffusion toward the bottom of the density of states in the conjugated polymer. Hence, for thin films, the excitations will be quenched before they have reached the redshifted sites to be emitted as PL.

ACKNOWLEDGMENTS

We are grateful to P. Bergman at Linköping University for help with the first time-resolved PL measurements and L. A. A. Pettersson, Linköping University, for the spectroscopic ellipsometry measurements. This work was financially supported by the Swedish Natural Science Research Council, the Swedish Research Council for Engineering Sciences (TFR), and the Carl Trygger Foundation.

¹N. S. Sariciftci and A. J. Heeger, *Int. J. Mod. Phys. B* **8**, 237 (1994).

²A. Ruseckas, M. Theander, L. Valkunas, M. R. Andersson, O. Inganäs, and V. Sundström, *J. Lumin.* **76&77**, 474 (1998).

³M. M.-L. Grage (unpublished).

⁴J. J. M. Halls, C. A. Walsh, N. C. Greenham, E. A. Marseglia, R. H. Friend, S. C. Moratti, and A. B. Holmes, *Nature* (London)

376, 498 (1995).

⁵A. Haugeneder, C. Kallinger, W. Spirkl, U. Lemmer, J. Feldmann, U. Scherf, E. Harth, A. Gügel, and K. Müllen, *SPIE* **3142**, 140 (1997).

⁶L. A. A. Petterson, L. S. Roman, and O. Inganäs, *J. Appl. Phys.* **86**, 487 (1999).

⁷L. Roman, W. Mammo, L. Petterson, M. Andersson, and O. In-

- ganäs, *Adv. Mater.* **10**, 774 (1998).
- ⁸N. S. Sariciftci, L. Smilowitz, A. J. Heeger, and F. Wudl, *Science* **258**, 1474 (1992).
- ⁹M. Theander, O. Inganäs, W. Mammo, T. Olinga, M. Svensson, and M. R. Andersson, *J. Phys. Chem. B* **103**, 7771 (1999).
- ¹⁰R. A. Marcus, *J. Chem. Phys.* **24**, 966 (1956).
- ¹¹D. Vacar, E. S. Maniloff, D. W. McBranch, and A. J. Heeger, *Phys. Rev. B* **56**, 4573 (1997).
- ¹²G. W. Heffner, D. S. Pearson, and C. L. Gettinger, *Polym. Eng. Sci.* **35**, 860 (1995).
- ¹³C. Schlebusch, B. Kessler, S. Cramm, and W. Eberhardt, *Synth. Met.* **77**, 151 (1996).
- ¹⁴S. B. Lee, A. A. Zakhidov, I. I. Khairullin, V. Y. Sokolov, P. K. Khabibullaev, K. Tada, K. Yoshimoto, and K. Yoshino, *Synth. Met.* **77**, 155 (1996).
- ¹⁵K. Hasharoni, M. Keshavarz-K, A. Sastre, A. Gonzáles, C. Bellavia-Lund, Y. Greewald, T. Swager, F. Wudl, and A. J. Heeger, *J. Chem. Phys.* **107**, 2308 (1997).